Molecular Phylogenetics and Evolution 53 (2009) 923–934

Contents lists available at ScienceDirect

Molecular Phylogenetics and Evolution

journal homepage: www.elsevier.com/locate/ympev

Evolutionary history of *Ramphastos* toucans: Molecular phylogenetics, temporal diversification, and biogeography

José S.L. Patané [a,*], Jason D. Weckstein [b], Alexandre Aleixo [c], John M. Bates [d]

[a] Departamento de Genética e Biologia Evolutiva, Instituto de Biociências, Universidade de São Paulo, Rua do Matão 277, CEP 05422-970 São Paulo/SP, Brazil
[b] Biodiversity Synthesis Center, The Field Museum of Natural History, 1400 S. Lake Shore Dr., Chicago, IL 60605-2496, USA
[c] Coordenação de Zoologia, Museu Paraense Emílio Goeldi, Caixa Postal 399, CEP 66040-170 Belém/PA, Brazil
[d] Department of Zoology, The Field Museum of Natural History, 1400 S. Lake Shore Dr., Chicago, IL 60605-2496, USA

ARTICLE INFO

Article history:
Received 17 March 2009
Revised 12 August 2009
Accepted 18 August 2009
Available online 20 August 2009

Keywords:
Ramphastos
Molecular phylogenetics
Bayesian dating
Amazonian biogeography
Neotropical avian evolution

ABSTRACT

The toucan genus *Ramphastos* (Piciformes: Ramphastidae) has been a model in the formulation of Neotropical paleobiogeographic hypotheses. Weckstein (2005) reported on the phylogenetic history of this genus based on three mitochondrial genes, but some relationships were weakly supported and one of the subspecies of *R. vitellinus* (*citreolaemus*) was unsampled. This study expands on Weckstein (2005) by adding more DNA sequence data (including a nuclear marker) and more samples, including *R. v. citreolaemus*. Maximum parsimony, maximum likelihood, and Bayesian methods recovered similar trees, with nodes showing high support. A monophyletic *R. vitellinus* complex was strongly supported as the sister-group to *R. brevis*. The results also confirmed that the southeastern and northern populations of *R. vitellinus ariel* are paraphyletic. *R. v. citreolaemus* is sister to the Amazonian subspecies of the *vitellinus* complex. Using three protein-coding genes (COI, cytochrome-*b* and ND2) and interval-calibrated nodes under a Bayesian relaxed-clock framework, we infer that ramphastid genera originated in the middle Miocene to early Pliocene, *Ramphastos* species originated between late Miocene and early Pleistocene, and intra-specific divergences took place throughout the Pleistocene. Parsimony-based reconstruction of ancestral areas indicated that evolution of the four *trans*-Andean *Ramphastos* taxa (*R. v. citreolaemus*, *R. a. swainsonii*, *R. brevis* and *R. sulfuratus*) was associated with four independent dispersals from the *cis*-Andean region. The last pulse of Andean uplift may have been important for the evolution of *R. sulfuratus*, whereas the origin of the other *trans*-Andean *Ramphastos* taxa is consistent with vicariance due to drying events in the lowland forests north of the Andes. Estimated rates of molecular evolution were higher than the "standard" bird rate of 2% substitutions/site/million years for two of the three genes analyzed (cytochrome-*b* and ND2).

1. Introduction

Toucans, araçaris, toucanets, and mountain-toucans (Piciformes, Ramphastidae) are among the most conspicuous and prominent symbols of the Neotropics (Galetti et al., 2000) and have attracted the attention of biologists since the onset of European exploration (Bates, 1863; Goeldi, 1894; Van Tyne, 1929, 1955; Gould and Rutgers, 1972; Haffer, 1974). Various authors (Haffer, 1974; Cracraft and Prum, 1988; Hackett and Lehn, 1997; Eberhard and Bermingham, 2005) have used members of this family as model taxa to construct generalized hypotheses of diversification patterns in the Neotropics. The toucan genus *Ramphastos*, widespread in the lowland Neotropics (Mexico south to Argentina), has been a focal taxon for understanding both the pattern and timing of Neotropical diversification. Previously to Haffer (1974), who postulated evolutionary relationships among the species of the genus *Ramphastos*, other authors had recognized up to 15 species (de Germiny, 1929; Peters, 1948; Meyer de Schauensee, 1966, 1970). Haffer (1974) recognized seven species-level taxa, dividing the genus into two groups differing in vocalization and bill shape: the channel-keel-billed "croakers" (*R. brevis*, *R. dicolorus*, *R. sulfuratus*, *R. toco*, and *R. vitellinus*) and the smooth-billed "yelpers" (*R. ambiguus* and *R. tucanus*). According to Haffer (1974), two of these species were considered monotypic (*R. brevis* and *R. dicolorus*), and the remaining five were polytypic.

Weckstein (2005) analyzed 2468 base pairs (bp) of DNA sequence data from three mitochondrial protein-coding genes (379 bp of COI, 1048 bp of cytochrome-*b*, and 1041 bp of ND2) using maximum parsimony (MP), maximum likelihood (ML), and Bayesian inference (BI) methods, for members of the seven biological species proposed by Haffer (1974), plus individuals belonging

* Corresponding author. Fax: +55 11 3726 7222, ramal 2014.
E-mail address: jspatane@yahoo.com (J.S.L. Patané).

1055-7903/$ - see front matter © 2009 Elsevier Inc. All rights reserved.
doi:10.1016/j.ympev.2009.08.017

to many subspecies of the polytypic taxa (*R. ambiguus ambiguus*, *R. a. swainsonii*, *R. sulfuratus sulfuratus*, *R. s. brevicarinatus*, *R. tucanus tucanus*, *R. t. cuvieri*, *R. vitellinus ariel*, *R. v. culminatus*, and *R. v. vitellinus*). Weckstein's (2005) phylogenetic analyses all converged on the same tree topology (Fig. 1). Some nodes exhibited bootstrap levels of less than 70% with MP and ML methods (though all showed Bayesian posterior probabilities $\geqslant 0.95$), including the node joining *R. brevis* with Amazonian *R. vitellinus* populations (northern *R. v. ariel* + *R. v. culminatus* + *R. v. vitellinus*). Similarly, the placement of *R. sulfuratus* and *R. dicolorus* were not corroborated by either MP-bootstrap (for *R. sulfuratus*) or ML-bootstrap support (for *R. dicolorus*).

Weckstein's (2005) tree is in agreement with Haffer's phylogenetic hypothesis in the following important ways: (1) yelpers were monophyletic; except for *R. toco*, (2) the croakers were monophyletic; (3) sympatric species with similar coloration (e.g., *R. brevis*/*R. a. swainsonii*; *R. v. culminatus*/*R. t. cuvieri*) were not sister taxa; and (4) six of the seven species proposed by Haffer (1974) were monophyletic. However, the monophyly of *R. vitellinus* ssp. was uncertain, as placement of *R. brevis* inside *R. vitellinus* ssp. was not ruled out, and the subspecies *R. v. ariel* was paraphyletic, with the southeastern (SE) *R. v. ariel* sister to a clade including all Amazonian *vitellinus* subspecies (Weckstein, 2005). The mtDNA paraphyly of *R. v. ariel* was not the first evidence that there are differences between these two disjunct *R. v. ariel* populations. Bill and wing lengths indicate that the disjunct southeastern population of *R. v. ariel* is slightly larger in body size (Haffer, 1974; Short and Horne, 2001). Another result obtained by Weckstein (2005) was an absence of reciprocal monophyly among subspecies of *R. tucanus* (*R. t. tucanus*/*R. t. cuvieri*) and among two subspecies of Amazonian *R. vitellinus* (*R. v. ariel* N/*R. v. culminatus*). Here, we further address the phylogenetic relationships of *Ramphastos* species using broader taxonomic sampling and an expanded DNA sequence data set, and infer lineage divergence dates to correlate the timing of diversification events in *Ramphastos* with biogeographic history.

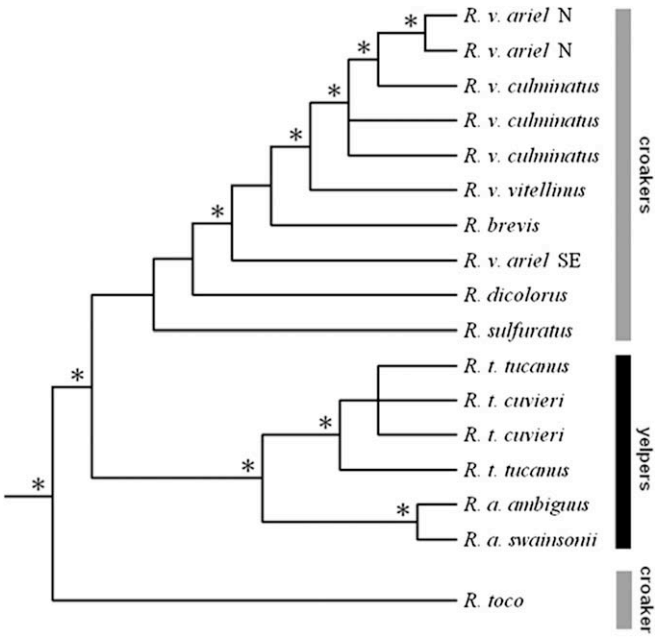

Fig. 1. Phylogeny depicting *Ramphastos* species relationships obtained by Weckstein (2005), based on the analysis of three mitochondrial genes (COI, cyt-*b* and ND2). Asterisks indicate branches that showed both bootstrap $\geqslant 70\%$ and posterior probability $\geqslant 95\%$.

2. Material and methods

2.1. Taxonomic sampling

We analyzed DNA sequences from 44 individuals, including *Ramphastos* specimens of 13 out of 16 currently recognized subspecies (Short and Horne, 2001) and outgroups. Twenty-six were the same individuals studied by Weckstein (2005; GenBank accessions for the three genes analyzed for each individual in that study are as follows: AY959799–AY959823, AY959825–AY959850, AY959852–AY959877, and AY959879). Two individuals of each taxon were studied in most cases (Table 1). Outgroup taxa included representatives of the four other genera in the family Ramphastidae (Lanyon and Zink, 1987; Prum, 1988; Höfling, 1998; Barker and Lanyon, 2000; Höfling and Alvarenga, 2001; Nahum et al., 2003; Moyle, 2004): *Selenidera reinwardtii*, *Aulacorhynchus prasinus*, *Andigena cucullata*, and *Pteroglossus inscriptus*. We also included *P. bailloni* because it was previously considered a separate monotypic genus, *Baillonius* (Kimura et al., 2004; see also Eberhard and Bermingham, 2005).

2.2. DNA amplification and sequencing

DNA was isolated from muscle tissue using a Dneasy tissue kit (Qiagen, Valencia, CA), except for *R. dicolorus* 1 and *R. v. ariel* SE 2 (blood), for which DNA was extracted using standard phenol:chloroform techniques (Sambrook and Russell, 2001), and the three *R. v. citreolaemus* specimens (museum toe pads) whose DNA was isolated using a Qiagen Microkit (Qiagen, Valencia, CA) with the addition of 10 mg/mL of DTT to the digestion buffer. All DNA isolation buffers contained 0.5 mg/mL proteinase K. We amplified and sequenced eight mitochondrial regions including 12S rRNA (12S), 16S rRNA (16S), a segment of the control region (D-loop), ATPases 6 and 8, cytochrome *c* oxidase subunit 1 (COI), cytochrome-*b* (cyt-*b*), nicotinamide adenine dinucleotide dehydrogenase subunit 2 (ND2) and one nuclear intron, β-fibrinogen intron 7 (fib-7). Amplification was done following Sambrook and Russell (2001) using Roche Taq, for a total of 35 cycles and annealing temperatures between 54 and 61 °C. Primers were either developed for the present study or else based on previous studies (Table 2). The 12S, cyt-*b* and ND2 genes were each amplified in two smaller overlapping pieces; these were compared to the sequence obtained from a single amplification of the whole gene, to check for potential amplification of paralogous copies. PCR-products were purified with either the Exonuclease and Shrimp Alkaline Phosphatase enzymatic reactions (United States Biochemical) or by cutting bands from a low melt agarose gel and digesting them with gelase (Epicentre Technologies, Madison, WI). Purified reactions were sequenced in both directions using amplification primers and dye-terminator chemistry (BigDye, Applied Biosystems), and the sequencing reactions were run on either ABI 377 or ABI 3730 sequencers.

We inferred ramphastid 12S secondary structure by comparison to an avian consensus structure (Espinosa de los Monteros, 2003); a region in the 3′ end, consisting of 122 bases, was excluded, because it was sequenced for only a few individuals. The final 12S alignment included only the loops and the 5′ portion of stems, to avoid the issue of rate covariation in stems. The 16S gene has no published prediction of secondary structure for birds, thus we used the entire sequenced region (except for ambiguous positions in the alignment). The D-loop segment corresponds to part of the central conserved domain including the Bird Box (2nd domain), plus part of the conserved sequence block or 3rd domain (Brown et al., 1986; Saccone et al., 1991; Pereira et al., 2004). D-loop sequences could not be obtained for the outgroup taxa except for the two

Table 1
Specimens used in this study.

index	Taxon ID[a]	Common name	Locality[b]	Source[c]	ID number
Ingroup					
1	*R. v. ariel* SE 1[d,e]	Ariel toucan	Brazil (São Paulo)	LSUMNS	B-35555
2	*R. v. ariel* SE 2[d]	Ariel toucan	Brazil (Santa Catarina)	LGEMA	R-213
3	*R. v. ariel* N 1[d,e]	Ariel toucan	Brazil (Pará)	LSUMNS	B-35667
4	*R. v. ariel* N 2[d,e]	Ariel toucan	Brazil (Pará)	LSUMNS	B-35668
5	*R. v. ariel* N 3	Ariel toucan	Brazil (Pará)	LSUMNS	B-35586
6	*R. v. citreolaemus* 1	Citron-throated toucan	Colombia (Antioquia)	FMNH	190822
7	*R. v. citreolaemus* 2	Citron-throated toucan	Colombia (Antioquia)	FMNH	190823
8	*R. v. citreolaemus* 3	Citron-throated toucan	Captive	FMNH	352027
9	*R. v. vitellinus* 1[d,e]	Channel-billed toucan	Brazil (Pará)	LSUMNS	B-35638
10	*R. v. vitellinus* 2[d]	Channel-billed toucan	Brazil (Pará)	LSUMNS	B-35646
11	*R. v. vitellinus* 3	Channel-billed toucan	Guyana (Iwokrama Reserve)	KU	B-1237
12	*R. v. culminatus* 1[d,e]	Yellow-ridged toucan	Brazil (Amazonas)	LSUMNS	B-35652
13	*R. v. culminatus* 2[d,e]	Yellow-ridged toucan	Brazil (Amazonas)	LSUMNS	B-35721
14	*R. v. culminatus* 3	Yellow-ridged toucan	Peru (Loreto)	LSUMNS	B-2860
15	*R. v. culminatus* 4	Yellow-ridged toucan	Peru (Loreto)	LSUMNS	B-7192
16	*R. v. culminatus* 5	Yellow-ridged toucan	Bolivia (La Paz)	LSUMNS	B-924
17	*R. t. tucanus* 1[d,e]	Red-billed toucan	Guyana (Iwokrama Reserve)	KU	B-1356
18	*R. t. tucanus* 2[d,e]	Red-billed toucan	Brazil (Pará)	LSUMNS	B-35550
19	*R. t. cuvieri* 1[d,e]	Cuvier's toucan	Brazil (Amazonas)	LSUMNS	B-35665
20	*R. t. cuvieri* 2[d,e]	Cuvier's toucan	Brazil (Amazonas)	LSUMNS	B-35666
21	*R. t. cuvieri* 3	Cuvier's toucan	Peru (Loreto)	LSUMNS	B-27691
22	*R. t. cuvieri* 4	Cuvier's toucan	Bolivia (Pando)	LSUMNS	B-9392
23	*R. toco* 1[d,e]	Toco toucan	Brazil (São Paulo)	LGEMA	R-264
24	*R. toco* 2[d]	Toco toucan	Brazil (São Paulo)	LGEMA	R-265
25	*R. toco* 3[d]	Toco toucan	Bolivia (Santa Cruz Zoo)	LSUMNS	B-1477
26	*R. toco* 4[d]	Toco toucan	Bolivia (Santa Cruz)	LSUMNS	B-38206
27	*R. a. swainsonii* 1[d,e]	Chestnut-mandibled toucan	Panama (Darién)	LSUMNS	B-2309
28	*R. a. swainsonii* 2[d]	Chestnut-mandibled toucan	Ecuador (Esmeraldas)	LSUMNS	B-11712
29	*R. a. ambiguus*[d,e]	Black-mandibled toucan	Ecuador (Zamora Chinchipe)	ANSP	4465
30	*R. dicolorus* 1[d,e]	Red-breasted toucan	Brazil (Santa Catarina)	LGEMA	R-210
31	*R. dicolorus* 2[d]	Red-breasted toucan	Paraguay (Caazapá)	KU	B-282
32	*R. s. sulfuratus*[d,e]	Keel-billed toucan	Mexico (Campeche)	KU	B-2007
33	*R. s. brevicarinatus*[d]	Keel-billed toucan	Panama (Colón)	LSUMNS	B-28577
34	*R. brevis* 1[d,e]	Choco toucan	Ecuador (Pichincha)	LSUMNS	B-12175
35	*R. brevis* 2[d]	Choco toucan	Ecuador (Pichincha)	LSUMNS	B-34977
Outgroup					
36	*Pteroglossus inscriptus*[d,e]	Lettered Araçari	Bolivia (Pando)	LSUMNS	B-8819
37	*Pteroglossus bailloni*[d]	Saffron toucanet	Paraguay (Caazapá)	LSUMNS	B-25891
38	*Selenidera reinwardtii*[d,e]	Golden-collared toucanet	Peru (Loreto)	LSUMNS	B-27756
39	*Andigena cucullata*[d,e]	Hooded Mountain Toucan	Bolivia (La Paz)	LSUMNS	B-1273
40	*Aulacorhynchus prasinus*[d]	Emerald toucanet	Panama (Darién)	LSUMNS	B-1373
41	*A. p. atrogularis*[e]	Black-throated toucanet	Peru (Madre de Dios)	LSUMNS	B-21201
42	*A. p. caeruleogularis*[e]	Blue-throated toucanet	Panama (Chiriquí)	LSUMNS	B-26403
43	*Semnornis frantzii*[e]	Prong-billed barbet	Costa Rica (Heredia)	LSUMNS	B-16019
44	*Semnornis ramphastinus*[e]	Toucan barbet	Ecuador (Pichincha)	LSUMNS	B-7771

[a] *A.* = *Aulacorhynchus*; *R.* = *Ramphastos*; *a.* = *ambiguus*; *s.* = *sulfuratus*; *t.* = *tucanus*; *v.* = *vitellinus*; N = northern distribution; SE = southeastern distribution.
[b] Detailed locality data have been deposited with sequences in GenBank.
[c] LGEMA = Laboratório de Genética e Evolução Molecular de Aves (Universidade de São Paulo-SP, Brazil); KU = University of Kansas Museum of Natural History; LSUMNS = Louisiana State University Museum of Natural Science; FMNH = Field Museum of Natural History; ANSP = Academy of Natural Sciences of Philadelphia.
[d] Samples used for phylogenetic analyses.
[e] Samples used for estimation of divergence dates.

Pteroglossus samples, therefore an additional outgroup sequence for this gene was obtained from GenBank, *Pteroglossus azara flavirostris* (NC_008549), to minimize the chance that we were aligning non-orthologous segments. The 10 bp overlap region of ATPase 6 and ATPase 8 was excluded from the data set to avoid the issue of correlation of states. These two genes were concatenated in a single data set ('ATPases') for further analyses, because the small size of the ATPase 8 alone (168 bp) prevented it from having its model parameters consistently estimated. We obtained sequences of fib-7 for all specimens except for *R. a. ambiguus* (ANSP 4465). All newly generated sequences are deposited in GenBank, with Accession Nos. GQ412306–GQ412335 (12S), GQ422968–GQ422997 (16S), GQ423027–GQ423053 (D-loop), GQ457940–GQ457969 (ATPases), GQ457970–GQ457984 (COI), GQ457985–GQ458001 (cyt-*b*), GQ458002–GQ458015 (ND2), and GQ422998–GQ423026 (fib-7).

2.3. Sequence analysis

We aligned forward and reverse strands for each specimen using Sequencher 4.7 (Gene Codes Corp.). For each partition (including the concatenated data set) we performed a multiple alignment using MEGA 3.0 (Kumar et al., 2004) with standard settings of the built-in Clustal algorithm. For each non-coding mtDNA gene (12S, 16S and D-loop), ambiguous sites were removed from alignments. These alignments were compared to others where the gap penalty varied and no ambiguous positions were discarded, to test if different alignments would alter the topology significantly.

A Chi-squared test for base composition homogeneity was run in PAUP* v4b10 (Swofford, 2003) for the concatenated data set, for each gene, and also for each codon position. We used only one specimen per taxon to minimize pseudoreplication (Hurlbert,

Table 2
Primers used for PCR and sequencing of toucan DNA samples. The asterisks indicate primers designed specifically for the *R. v. citreolaemus* toe pad samples.

Genic region	Direction	Primer name	Primer sequence	Source
12S:	L	*Lphe1248*	5′-AAA GCA TGG CAC TGA AGA YGC	Tavares, E. S. (pers. comm.)
	H	*12SH1843*	5′-CCG CCA AGT CCT TAG AGT TT	Tavares, E. S. (pers. comm.)
	L	*12SL1735*	5′-GGA TTA GAT ACC CCA CTA TGC	Miyaki et al. (1998)
	H	*12SH2170*	5′-AGG GTG ACG GGC GGT ATG TAC G	Miyaki et al. (1998)
16S:	L	*16SL2702*	5′-CCT ACC GAG CTG GGT GAT AGC TGG TT	Miyaki et al. (1998)
	H	*16SH3309*	5′-TGC GCT ACC TTC GCA CGG T	Miyaki et al. (1998)
D-loop:	L	*L538*	5′-CCT CTG GTT CCT ARG TCA GG	Modified from Delport et al. (2002)
	H	*PROHSS*	5′-GCT TTG GGA GTT GGA GAT AAA GG	Cabanne, G. S. (pers. comm.)
ATPases 6 and 8:	L	*CO2GQL*	5′-GGA CAA TGC TCA GAA ATC TGC GG	González et al. (2003)
	H	*A6TPHRV*	5′-ATT GAT AGT TGY GTT GTT GGG GT	Present study
	L	*ATPaseLintA*	5′-CCA AAC ARC TAA TRC TRC C	Present study
	H	*CO3HMH*	5′-CAT GGG CTG GGG TCR ACT ATG TG	Eberhard and Bermingham (2004)
COI:	L	*L6625*	5′-CTA GAG GAG CCT GTT CTA TAA TCG	Hafner et al. (1994)
	H	*H7005*	5′-CTT TCA GGT GTA AGC TGA RTG C	Hafner et al. (1994)
Cyt-*b*:	L	*L14841*	5′-GCT TCC ATC CAA CAT CTC AGC ATG ATG	Kocher et al. (1989)
	H	*TOUCCBH*	5′-GAG AAR RAT GGG TGR AAT GG	Weckstein (2005)
	L	*TOUCCBL*	5′-CTT CCT NCT NCC ATT CCT AAT YRC AGG	Weckstein (2005)
	H	*H16065*	5′-GGA GTC TTC AGT CTC TGG TTT ACA AGA C	Helm-Bychowski and Cracraft (1993)
	L	*CBL15845RV**	5′-CTC CRC CTC ACA TTA AAC CCG	Modified from Ribas et al. (2005)
	H	*CBH15120RV**	5′-GRA GAT TGC GGA TTA GTC AGC CA	Modified from Ribas et al. (2005)
	L	*CBL15062RV**	5′-CCG CAG ACA CCT CCY TAG CC	Modified from Ribas et al. (2005)
	H	*CBH15315RV**	5′-GTA ATG ACR GTG GCG CCT CAG	Modified from Ribas et al. (2005)
	H	*CBH15902RV**	5′-ACA GGT TGG CTT CCT ACT CAR G	Modified from Ribas et al. (2005)
ND2:	L	*L5215*	5′-TAT CGG GCC CAT ACC CCG AAA AT	Hackett (1996)
	H	*H5776TOUC*	5′-GGC TGA RYA GGC MTC AAC CAR AC	Weckstein (2005)
	L	*L5758TOUC*	5′-TGN GAG ATR GAG GAG AAR GC	Weckstein (2005)
	H	*H6313*	5′-CTC TTA TTT AAG GCT TTG AAG GC	Sorenson et al. (1999)
Fib-7:	L	*FibL2*	5′-CTT CTG AGT AGG CAG AAC TT	Moyle (2004)
	H	*Fib-BI7U*	5′-GGA GAA AAC AGG ACA ATG ACA ATT CAC	Prychitko and Moore (1997)

1984), and discarded the invariant sites (Cunningham, 1997). The ILD test (Farris et al., 1994) as implemented in PAUP* was used to assess congruence among the different partitions, using RELL sampling for a total of 1000 random permutations. Saturation plots for each gene were obtained by comparing the ML-patristic distances to the uncorrected genetic distances (*p*-distances). For a quantitative appraisal of genetic differences, the *p*-distances within and among *Ramphastos* species and subspecies were calculated.

2.4. Phylogenetic analysis

MP estimation for each DNA region and for the concatenated data set was done in PAUP*, using exact search by the branch-and-bound method, with indels considered either as missing data, or as a fifth state in a subsequent analysis. The MP-bootstraps were implemented using 10 random addition cycles and 1000 pseudoreplicates, with heuristic search.

The best model for each partition and for the concatenated data set was chosen by the corrected Akaike information criterion (AICc) in Modeltest 3.7 (Posada and Crandall, 1998), including the number of branches as free parameters, and considering sample size as the number of characters times the number of taxa (Modeltest 3.7 manual; Posada and Buckley, 2004). ML analysis of the concatenated data set was done in PAUP*, with an initial search using model parameter values provided by Modeltest, then parameters were re-estimated using the resulting tree, and the process was repeated until the same tree and parameter values were recovered in successive iterations. ML-bootstraps were calculated in Treefinder (Jobb et al., 2004), using 1000 pseudoreplicates. We performed separate MP and ML analyses for the cyt-*b* data set alone which included the three partial *R. v. citreolaemus* cyt-*b* sequences. The general procedures for model choice, MP and ML estimates, and associated bootstrap values were the same as described above.

Three different partition strategies were implemented for Bayesian analyses in MrBayes 3.1 (Ronquist and Huelsenbeck, 2003): five-partition (D-loop + 12S + 16S + coding genes + fib-7), seven-partition (D-loop + 12S + 16S + 1st codon pos. + 2nd codon pos. + 3rd codon pos. + fib-7), and a six-partition design excluding the fib-7 intron (D-loop + 12S + 16S + 1st codon pos. + 2nd codon pos. + 3rd codon pos.). Topologies were linked across partitions, using the same models as in the ML analyses, or a slightly overparametrized model, as suggested when the exact model chosen by Modeltest cannot be input into MrBayes (Huelsenbeck and Ronquist, 2005). Model parameters and priors varied independently across partitions. We ran four different MrBayes analyses, each with two parallel simultaneous runs, with each parallel run including one cold chain and three heated chains, for a total of 5×10^6 generations each. For all phylogenetic analyses, it was assumed that reasonable node support values for the bootstrap and Bayesian posterior probability (PP) were at least $\geqslant$70% and $\geqslant$95%, respectively.

We performed two additional phylogenetic tree searches, one including all *R. vitellinus* ssp. samples (samples 1–16 in Table 1; *R. v. ariel* SE as outgroup), and another including all *R. tucanus* ssp. samples (samples 17–22 in Table 1; *R. ambiguus* ssp. as outgroup, samples 27–29). Both analyses were based on reduced mtDNA data sets composed of only protein-coding genes. Search and bootstrap options were the same as previously described. These searches were valuable for addressing the evolutionary history of well marked Amazonian *Ramphastos* forms and related biogeographic events.

2.5. Biogeographic analysis

We used a parsimony-based approach to perform ancestral area reconstructions for supported nodes in the combined-data phylogeny (including *R. v. citreolaemus* based on its position in the cyt-*b* data set) using Mesquite v.2.6 (Maddison and Maddison, 2009). Distribution areas of terminals were coded as either *cis*-Andean (encompassing all areas from the eastern slope of the Eastern Andean Cordillera eastwards), including the taxa *R. dicolorus*, *R. toco*,

R. tucanus ssp., *R. a. ambiguus*, and *R. vitellinus* ssp. (excluding *citreolaemus*); or *trans*-Andean (encompassing all areas from the western slope of the Eastern Andean Cordillera westwards), including *R. brevis*, *R. sulfuratus*, *R. a. swainsonii*, and *R. v. citreolaemus*.

2.6. Dating divergences

We performed a Bayesian relaxed-clock analysis in BEAST v1.4.8 (Drummond and Rambaut, 2007) to assess species divergence times using the COI, cyt-*b*, and ND2 genes. Only one individual per taxon was used except for *R. v. culminatus*, *R. v. ariel* N, *R. t. cuvieri*, and *R. t. tucanus* samples, which did not show reciprocal monophyly (see Table 1 for samples used in this analysis). We also included sequences of two pairs of sister taxa, *Semnornis frantzii*/*S. ramphastinus* and *Aulacorhynchus prasinus atrogularis*/*A. p. caeruleogularis* (GenBank Accessions EU285703 and EU285777) to calibrate maximum divergence times within the *Ramphastos* tree. The formation of the isthmus of Panama around 3.00–3.95 Ma (Saito, 1976; Keigwin, 1978, 1982; Duque-Caro, 1990; Coates et al., 1992; Ibaraki, 1997, 2002) might have allowed dispersal of these taxa from South America to Central America, but we believe that the rapid uplift of the Talamanca highlands of Costa Rica and western Panama at about 4.5 Ma (Abratis and Worner, 2001; Grafe et al., 2002) is a more conservative maximum age constraint, justified by the fact that both *Semnornis* and *Aulacorhynchus* taxa used here are extant highland taxa. Thus we set the age priors as Uniform [0.0, 4.5] Ma for these calibrated nodes.

We implemented an uncorrelated lognormal model for rates (Drummond et al., 2006), with the rate at each branch independently drawn from a lognormal distribution. The mean (parameter ucld.mean) for this lognormal was treated as an unknown parameter following a Normal distribution [$\mu = 1.105\%$; $\sigma = 0.34\%$] substitutions/site/branch/Ma (s/s/b/a). These parameter values correspond to a Normal [$\mu = 2.21\%$; $\sigma = 0.68\%$] s/s/Ma approximately (s/s/Ma is the unit of measure most commonly reported for rates in the literature; the farther rates are from clock-like, the more inaccurate the approximation). This rate distribution prior was based on a study by Weir and Schluter (2008), who performed a cross-validation analysis on a data set that included multiple Neotropical avian lineages. Although their study was based on cyt-*b* alone, we employed the same ucld.mean prior (Normal [$\mu = 1.105\%$; $\sigma = 0.34\%$]) for cyt-*b*, COI and ND2 in our analysis, assuming this prior range is broad enough to represent the variability in rate for these mtDNA protein-coding genes. For the standard deviation of rates in the uncorrelated lognormal model (parameter ucld.stdev) we used a Uniform [0, 10] s/s/b/Ma prior for each of the three genes. Each gene had its own reversible model, and each had its own ucld.mean and ucld.stdev parameters, both following the priors above. The topology was fixed among partitions and not allowed to change during the run, except for the lineages that showed paraphyly (*R. v. culminatus*/*R. v. ariel* N and *R. t. cuvieri*/*R. t. tucanus*). The prior on the non-calibrated node ages was a Birth–Death process (Gernhard, 2008), with default parameters. The bounds relative to the parameters "meanRate" (the estimated number of substitutions per site across the whole tree divided by the estimated length of the whole tree in time), "coefficientOfVariation" (the ratio ucld.stdev/ucld.mean), and "covariance" (which measures autocorrelation of rates on the phylogeny) were all set to Uniform in the ranges [0, 10], [0, 10], and [−10, 10], respectively. Models for the three genes under this relaxed-clock data set were obtained from Modeltest, with relative substitution parameters following a Uniform [0, 100]. The gamma distribution of rates across sites (with four discrete rate categories) and proportion of invariant sites followed Uniform distributions within [0, 100] and [0, 1], respectively. We ran BEAST for 10,000,000 generations and sampled output every 1000th generation.

The parameter used to report posterior rates was meanRate instead of ucld.mean, because the ucld.mean parameter does not take into account the fact that some branches are longer than others (BEAST 1.4.8 manual). Thus, reported posterior rates can be higher than the upper limit for the ucld.mean parameter. Stationarity of the chains and the effective sample size (ESS) for each parameter were checked with Tracer v1.4.1 (Rambaut and Drummond, 2008), which also summarizes the posterior range of parameters using a 95% HPD (highest posterior density) interval. Association of divergence time intervals with their respective geologic periods followed Gradstein et al. (2004).

We also tested whether the posterior ranges were sensitive to distributional assumptions by setting different priors for: (1) the calibrated nodes including the two *Semnornis* species split and the two *Aulacorhynchus* subspecies split concomitantly (exponential, normal, lognormal, or gamma, using 0.0 as a hard bound on the minimum age, and 4.5 as an upper soft bound instead of a Uniform [0, 4.5]); and (2) the substitution rate parameters of all genes (Jeffreys distribution, instead of Uniform [0, 100]).

3. Results

3.1. Sequence attributes

For tissue samples, we obtained individual sequences between 833–846 bp for the 12S, 390–564 bp for the 16S, 356–710 bp of the D-loop, the entire ATPase 6 and 8 genes (842 bp, with further removal of the 10 bp overlap region), 379 bp of COI, 1048 bp of cyt-*b*, the entire ND2 (1041 bp), and 380 bp of fib-7. The 16S, D-loop, COI and fib-7 regions each were amplified using a single pair of primers; the other genes were amplified using different primer combinations, generating two fragments (12S, cyt-*b*, ND2), or a single fragment (ATPases 6 + 8; Table 2). For the *R. vitellinus citreolaemus* toe pad samples, we obtained only a portion (549–652 bp) of the cyt-*b* gene, using the same external primers as other samples (Table 2) and internal primers designed from an alignment of *R. vitellinus* ssp. samples alone. We consider the sequences we generated to be orthologous because: (1) the data were gathered mostly from mitochondria-rich tissues, except for *R. dicolorus* 1 and *R. v. ariel* SE 2 (blood); (2) no substitutions or indels were detected when assembling the two complementary strands for the same individual; (3) for genes amplified in two separate smaller fragments, at least one individual had its DNA amplified and sequenced as a single large fragment, perfectly matching the sequences of the smaller fragments; (4) no premature stop-codons or reading frame shifts were detected in the coding genes.

For the non-coding genes, there were minor MP-bootstrap differences among trees derived from alignments with gap penalties of 7.5, 15.0, and 30, or with the default Clustal parameter values (gap penalty = 15) plus manual exclusion of ambiguous positions; hence we chose the latter as the standard alignment procedure for each non-coding gene. Alignment sizes for all regions studied were as follows: 12S – 628 bp; 16S – 546 bp; D-loop – 699 bp; ATPase 6 – 674 bp; ATPase 8 – 158 bp; COI – 379 bp; cyt-*b* – 1048 bp; ND2 – 1041 bp; fib-7 – 380 bp. The concatenated data set had a total of 5553 bp, with 3903 of the characters constant, 396 characters autapomorphic, and 1254 characters parsimony-informative (in the analysis considering gaps as a fifth state).

The Chi-square test of base frequencies indicated no significant differences, either for the concatenated alignment, for each gene separately, or at different codon positions in coding genes ($P > 0.05$ for all). The ILD test did not indicate significant differences in the phylogenetic signal among the nine different partitions ($P = 0.705$), and thus we concatenated these partitions for combined analysis. Plots including ingroup and outgroup

comparisons indicated that for all DNA regions saturation of *p*-distances began at approximately 12% (for 12S) to 18% (for ND2) substitutions/site (data not shown).

3.2. Genetic distances

p-Distances were calculated using the mtDNA protein-coding genes combined (Table 3). The highest mean intra-specific *p*-distance (1.31%) was for the species *R. vitellinus*. The inter-taxonomic range of *p*-distances between specimens of *R. v. culminatus* and *R. v. ariel* N broadly overlapped the intra-taxonomic range for these same taxa (Table 3). This same pattern was observed for *R. tucanus* ssp., with intra-taxonomic distances in *R. t. tucanus* and *R. t. cuvieri* overlapping their inter-taxonomic comparisons (Table 3).

3.3. Phylogenetic results

Substitution models chosen for each region (acronyms according to Modeltest 3.7) included GTR+I+G for 12S and 16S, TrN+I+G for ATPases and cyt-*b*, TrN+G for ND2, HKY+I+G for COI, HKY+I for D-loop, and HKY for fib-7. The combined data set model was GTR+I+G. Separate analyses of each gene region varied in the corroboration of nodes present in the tree derived from the combined data set (Table 4). Fib-7 showed the least resolution among all DNA regions, resolving only the monophyly of *R. vitellinus* ssp. For each gene, the number of nodes supported by high bootstrap values ($\geqslant$ 70%) was generally higher for ML than for MP (Table 4).

Both MP-bootstrap analyses (gaps treated as fifth state, gaps treated as missing data) produced similar support values (further MP references in the text, tables and figures referring to the "fifth state" analysis). MP, ML and BI topologies based on the combined data set were similar. The ML tree (Fig. 3a) with MP-bootstrap, ML-bootstrap, and PP values for the seven-partition Bayesian analysis (which were similar to values obtained from five- and six-partition Bayesian schemes; data not shown) shows that individuals of the same taxon always formed monophyletic units, except for the two *R. tucanus* ssp. and two of the Amazonian *R. vitellinus* ssp. (*culminatus* and *ariel* N). The resulting topology is largely consistent with that of Weckstein (2005); however, the position of *R. brevis* has been resolved as sister to a clade containing all *R. vitellinus* ssp. (Fig. 3a). In the ML analysis of the cyt-*b* data set including *R. v. citreolaemus* (Fig. 3b), the position of this taxon as sister to the Amazonian *R. vitellinus* ssp. (*R. v. vitellinus*, *R. v. culminatus*, and *R. v. ariel* N) is strongly corroborated by MP-bootstrap and ML-bootstrap values.

Table 3
p-Distances within *Ramphastos* sp. based on the mtDNA protein-coding data set (ATPases + COI + cyt-*b* + ND2).

	Mean (%)	Range (%)
Within Ramphastos sp.		
R. vitellinus	1.31	
R. ambiguus	0.92	
R. sulfuratus	0.47	
R. tucanus	0.35	
R. toco	0.24	
R. dicolorus	0.24	
R. brevis	0.03	
R. vitellinus ssp.		
Intra-taxonomic		
R. v. ariel SE	0.27	–
R. v. citreolaemus	0.18	0.182–0.184
R. v. vitellinus	0.21	0.12–0.28
R. v. culminatus	0.22	0.12–0.32
R. v. ariel N	0.22	0.16–0.24
culminatus + *ariel* N	0.25	0.12–0.48
Inter-taxonomic[a]		
ariel SE × others[b]	2.78	2.31–3.07
citreolaemus × others[c]	1.72	1.39–2.09
vitellinus × others[d]	0.60	0.40–0.73
culminatus × *ariel* N	0.28	0.12–0.48
Yelpers		
Intra-taxonomic		
R. ambiguus	0.92	0.06–1.35
R. tucanus	0.35	0.09–0.61
Inter-taxonomic		
R. ambiguus × *R. tucanus*	4.52	4.32–4.81
R. tucanus ssp.		
Intra-taxonomic		
R. t. tucanus	0.46	–
R. t. cuvieri	0.32	0.13–0.48
Inter-taxonomic		
tucanus × *cuvieri*	0.36	0.09–0.61
R. ambiguus ssp.		
Intra-taxonomic		
R. a. ambiguus	–	–
R. a. swainsonii	0.06	–
Inter-taxonomic		
ambiguus × *swainsonii*	1.35	1.345–1.346

[a] *p*-Distances between reciprocally monophyletic groups, except for *culminatus* × *ariel* N (see Fig. 3).
[b] clade [*R. v. citreolaemus* + *R. v. vitellinus* + *R. v. culminatus* + *R. v. ariel* N].
[c] clade [*R. v. vitellinus* + *R. v. culminatus* + *R. v. ariel* N].
[d] clade [*R. v. culminatus* + *R. v. ariel* N].

3.4. Biogeographic analyses

The most parsimonious reconstruction of ancestral areas indicated that the evolution of the four *trans*-Andean clades (*R. a. swainsonii*, *R. brevis*, *R. sulfuratus* and *R. v. citreolaemus*) is associated with four independent dispersals from the *cis*-Andean region (Fig. 4). In the consensus ML tree obtained with all *R. vitellinus* ssp. samples (Fig. 5a), only the portion of the tree depicting the relationship among Amazonian samples is shown, with their respective areas of distribution. The tree including all *R. tucanus* ssp. samples had no resolution (not shown).

3.5. Divergence estimates

For each independent run, a burn-in of 1% of the total number of generations was sufficient for parameters to show stationarity. ESSs for all parameters were >200. Five BEAST analyses, each differing in the divergence distribution prior (uniform, exponential, normal, lognormal, and gamma) were conducted for the two calibration points. We focus on the analysis using the uniform prior for calibrated ages, because it puts equal weight on splitting events throughout the prior distribution range without incorporating further assumptions; furthermore, the use of a uniform prior had almost the same precision (in terms of posterior 95% region sizes of the nodes dated) and accuracy (as its posterior 95% regions overlapped mostly the same ranges as other priors) as any other prior distribution. We acknowledge that different combinations of parameter values could alter the shape of the lognormal and gamma distributions and still include the same soft bounds previously mentioned, but for the sake of generality we assumed that the combinations used here (lognormal: $\mu = 0.6816$, $\sigma = 0.5$, offset = 0.0; gamma: $\alpha = 2.0$, $\beta = 0.9485$, offset = 0.0) are representative of reasonable prior age intervals. Regarding substitution rate parameters, using a Jeffreys prior, rather than a uniform prior, also had negligible effects on posterior divergence intervals, again indicating that biases due to different prior assumptions are unlikely to affect interval age estimates for our data set. A tree with divergence times and associated 95% intervals was obtained (Fig. 6). Posterior rate estimates (parameter 'meanRate' in BEAST) ranged

Table 4
Nodes present in the phylogenetic tree constructed from the entire concatenated data set (see Fig. 3a). Nodes supported by analyses of individual data partitions with ⩾70% bootstrap values are noted with gray shading for MP and/or an 'X' for ML. "Non-coding" and "Coding" data sets were analyzed by ML only.

Branches supported	12S	16S	D-loop	ATPases	COI	Cyt-b	ND2	fib-7	Non-coding	Coding
R. toco / [croakers+yelpers]				x			x			x
croakers / yelpers										x
croakers (monophyly)				x						x
R. sulfuratus / [*R. dicolorus* + *R. brevis* + *R. vitellinus* ssp.]										x
R. dicolorus / [*R. brevis* + *R. vitellinus* ssp.]							x			x
R. brevis + *R. vitellinus* ssp. (monophyly)	x		x	x	x	x	x		x	x
R. brevis / *R. vitellinus* ssp.			x			x			x	
R. vitellinus ssp. (monophyly)			x			x		x	x	
R. v. ariel SE / [*R. v. vitellinus* + *R. v. culminatus* + *R. v. ariel* N]			x			x			x	
Amazonian *R. vitellinus* ssp. (monophyly)	x	x	x	x	x	x	x		x	x
R. v. vitellinus / [*R. v. culminatus* + *R. v. ariel* N]				x		x				x
R. v. culminatus + *R. v. ariel* N (monophyly)				x		x	x			x
R. v. culminatus 2 / [*R. v. culminatus* 1 + *R. v. ariel* N 1 + *R. v. ariel* N 2]						x				x
yelpers (monophyly)		x	x	x		x	x		x	x
R. ambiguus ssp. / *R. tucanus* ssp.		x	x	x		x	x		x	x
R. ambiguus ssp. (monophyly)	x	x	x	x	x	x	x		x	x
R. a. ambiguus / *R. a. swainsonii*	x	x	x	x	x	x	x		x	x
R. tucanus ssp. (monophyly)	x	x	x	x	x	x	x		x	x
R. t. tucanus 1 / [*R. tucanus* 2 + *R. t. cuvieri* 1 + *R. t. cuvieri* 2]	x		x	x	x		x		x	
Total in agreement (ML)	6	6	11	12	6	13	11	1	11	15
Total in agreement (MP)	4	6	6	10	4	13	11	1	-	-

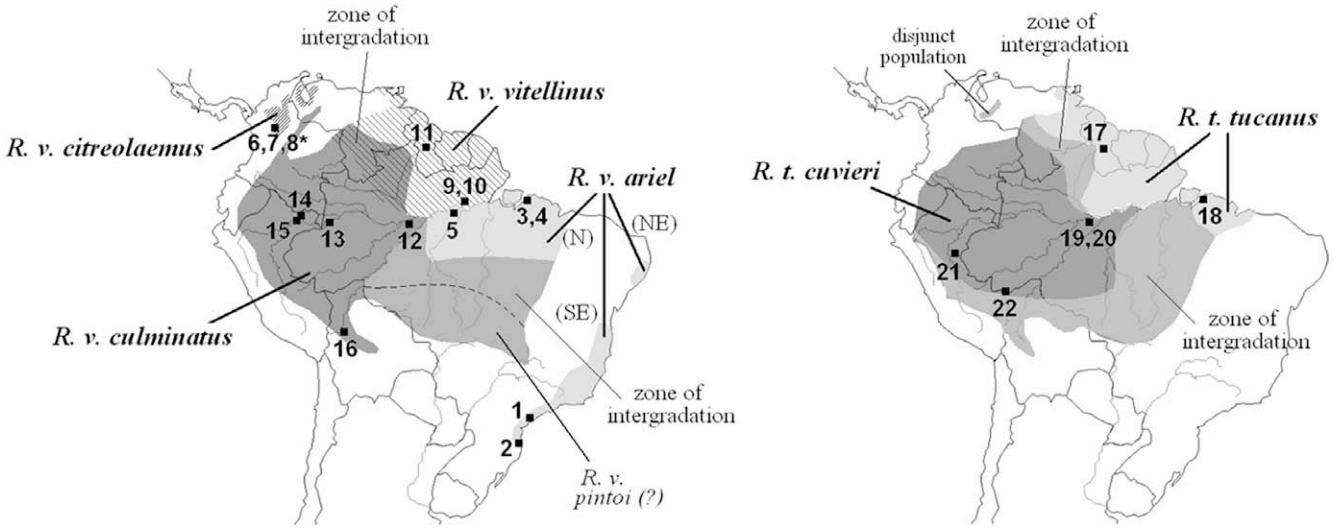

Fig. 2. Distribution and sample locations of *R. vitellinus* ssp. (left) and *R. tucanus* ssp. (right). The numbers refer to the indexes in Table 1. The question mark indicates a population of disputed taxonomic status (*R. v. pintoi*). The asterisk indicates that specimen #8 was a captive bird and thus the specific locality of origin of this specimen is unknown.

from 1.68% to 2.93% s/s/Ma for COI, 2.42–3.65% for cyt-*b*, and 2.72–4.10% for ND2.

4. Discussion

4.1. Phylogenetic relationships

Weckstein (2005) did not find strong support for the phylogenetic position of *R. dicolorus* and *R. sulfuratus* (Fig. 1). Our study corroborated the phylogenetic relationships of these taxa with stronger MP- and ML-bootstrap and PP support (Fig. 3a). Weckstein (2005) also found equivocal support for the monophyly of *R. vitellinus* subspecies, which could be either a sister clade to *R. brevis*, or paraphyletic with respect to *R. brevis*. Our analyses strongly supported the monophyly of *R. vitellinus* (Fig. 3a and b). This was also true in the analysis of the nuclear intron fib-7 alone (Table 4). Weckstein (2005) used a single sample of *R. v. ariel* from the southeastern Atlantic Forest region (*R. v. ariel* SE). Inclusion of an additional *R. v. ariel* SE sample in the present study still supported this taxon as sister to all other *R. vitellinus* ssp. (Fig. 3a and b). *R. v. citreolaemus* was strongly supported as the sister-group to the Amazonian *R. vitellinus* ssp. (Fig. 3b). Within Amazonian subspecies, *R. v. vitellinus* was sister to a monophyletic clade composed of *R. v. culminatus* and *R. v. ariel* N, but within this clade subspecies were not monophyletic. The overlap of inter-taxonomic *p*-distances between *R. v. culminatus* and *R. v. ariel* N and their respective intra-group distances agreed with the phylogenetic results, indicating that these may not be independent evolutionary

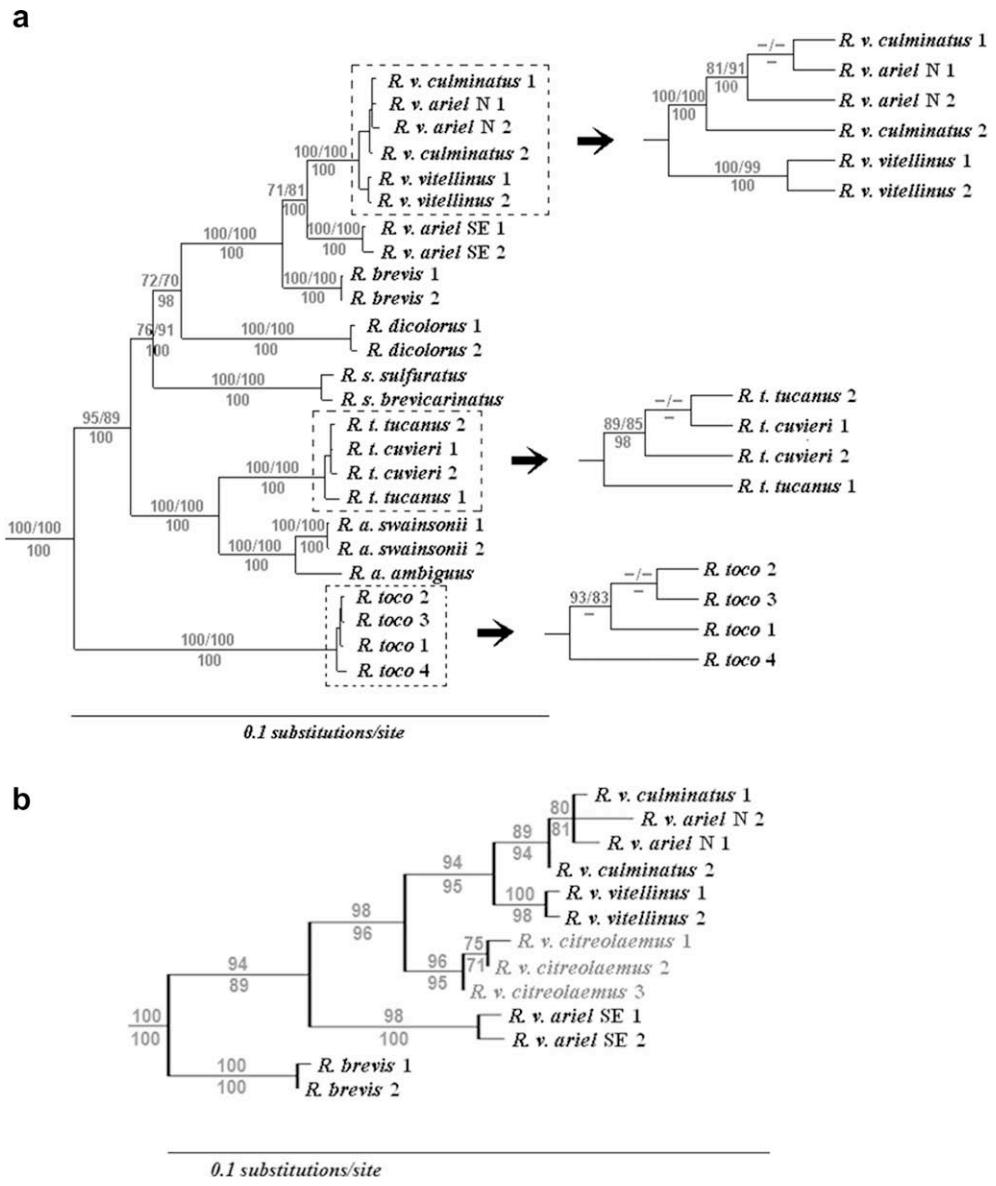

Fig. 3. Phylogenetic trees constructed with: (a) the combined data set analysis (model = GTR+I+G; lnL = −21999.74); and (b) a portion of the topology obtained by analysis of the cyt-*b* data alone, including the three *R. v. citreolaemus* samples (model = TrN+I+G; lnL = −4771.30). Values on branches in (a) indicate bootstrap values for MP (top left) and ML (top right) and posterior probabilities (below). Values on branches in (b) indicate ML (above) and MP (below) bootstrap values.

units. The same was true for the genetic distances and phylogenetic comparisons of the two *R. tucanus* subspecies, *R. t. tucanus* and *R. t. cuvieri*. Therefore, our study found no molecular evidence for the differentiation of *R. tucanus* ssp., or the *R. v. culminatus*/*ariel* N clade; more comprehensive sampling is needed to understand the population limits of these two *Ramphastos* groups.

4.2. Biogeography and dating of diversifications

Our results indicate the *Semnornis*/Ramphastidae split took place during the late to middle Miocene (10.27–15.66 Ma), much more recently than the estimate of the origin of Ramphastidae by Nahum et al. (2003) of 73.0–92.2 Ma. We believe that our estimates are more reasonable because Nahum et al. (2003) rooted their tree with *Gallus gallus* (an ancient split within neognathes; Hackett et al., 2008), which may be problematic due to saturation, and also because they used a linearized tree method with no correction for rate heterogeneity throughout the phylogeny. We find that ramphastid genera evolved in the Miocene (including the genus *Ramphastos*, 8.58–13.02 Ma), with the *Selenidera*/*Andigena* split interval bar reaching into the early Pliocene (Fig. 6). These dates coincide with the timing of events such as the uplift of southern portions of the Andes (Farías et al., 2008), the increased drying of a huge lake complex in Amazonia (the Pebas/Solimões formation or Lake Pebas; Wesselingh et al., 2001; Hovikoski et al., 2007), and a gradual increase in open vegetation areas as extrapolated from the spreading of C_4 grasslands (Nambudiri et al., 1978; Latorre et al., 1997; Jacobs et al., 1999). Expansion of open vegetation in the late Miocene may be associated with the evolution of *R. toco* (3.69–5.86 Ma), the only *Ramphastos* species occupying open habitats.

Diversification of *Ramphastos* species includes the evolution of four *trans*-Andean taxa (*R. sulfuratus, R. brevis*, *R. v. citreolaemus* and *R. a. swainsonii*). Our results support four independent dispersal events driving the evolution of these clades (Fig. 4). The origin of *R. sulfuratus* (2.60–4.15 Ma) may be associated with vicariant events such as sea transgressions of up to ~100 m in the late Tertiary and/or with the last Andean uplift pulse (2.7–5 Ma; Nores,

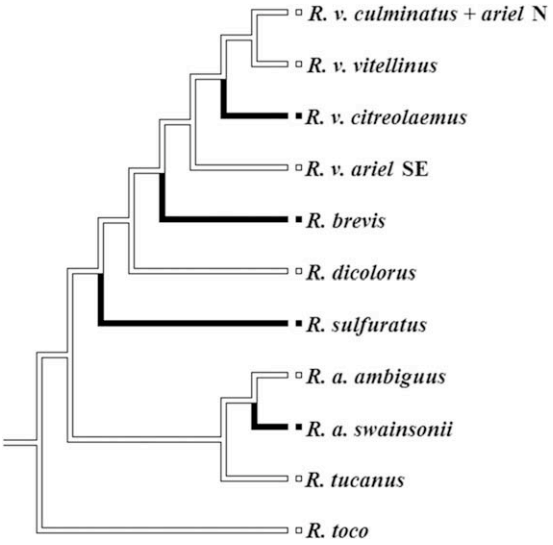

Fig. 4. Parsimony-based reconstruction of ancestral areas of distribution. White squares indicate *cis*-Andean, and black squares indicate *trans*-Andean distribution. Branches are colored according to the most parsimonious reconstruction.

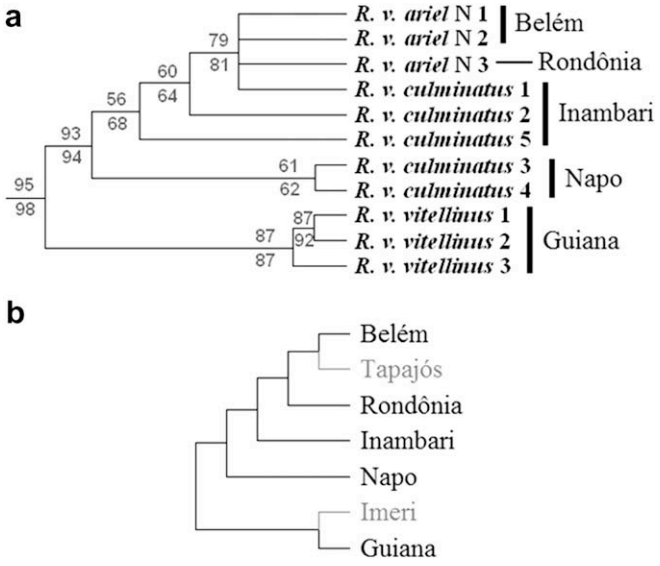

Fig. 5. (a) Phylogeny of Amazonian *R. vitellinus* ssp. with all samples from Table 1, based on protein-coding genes (ATPases + COI + cyt-*b* + ND2). ML-bootstraps (above branches) and MP-bootstraps (below branches) are displayed. *R. v. ariel* SE and *R. v. citreolaemus* were used as outgroups. Areas of endemism from which each specimen (and thus haplotype) was collected are indicated. (b) Relationships among Amazonian areas of endemism based on parsimony analysis of endemicity of many non-passerine lineages (Borges, 2007); areas in gray represent regions for which no *Ramphastos* specimens were analyzed.

2004), but is not likely to be associated with the late Tertiary glaciation cycles (which started ~2.6 Ma), thus not supporting the hypothesis that dryer habitats separated populations due to glacial periods (Haffer, 1997). However, dryer regions during glacial periods isolating *trans*-Andean areas of endemism from those of western Amazonia may be a plausible vicariant scenario for the origin of *R. brevis* (0.99–1.75 Ma), *R. a. swainsonii* (0.33–0.81 Ma), and *R. v. citreolaemus* (0.20–1.40 Ma, see below).

The phylogenetic origin of *R. vitellinus* ssp. suggests a relatively complex historical scenario from a presumably widespread ancestor. Its members are distributed in Amazonia (*R. v. vitellinus*, *R. v. culminatus* and *R. v. ariel* N), the *trans*-Andean region (*R. v. citreolaemus*), and Atlantic forest (*R. v. ariel* SE). The basal split was between *R. v. ariel* SE and the remaining (northern) forms (0.77–1.40 Ma). The most common recent ancestor of all the extant *R. vitellinus* ssp. may have existed as a non-disjunct population that was separated by a vicariant event between Atlantic forest and northern regions, a pattern also detected in other Neotropical avian lineages such as species in the genus *Tangara* (Burns and Naoki, 2004). Botanical (Bigarella et al., 1975; Andrade-Lima, 1982; Mori, 1989) and faunistic (Bigarella et al., 1975; Willis, 1992; Bates et al. 1998; Costa, 2003) similarities suggest multiple connections of Atlantic forest and Amazonia in the past. This view is reinforced by paleopalinological (De Oliveira et al., 1999) and geological (Auler et al., 2004) data, suggesting that periodic forested links existed between them at least during the Pleistocene, and may have varied in location as well as in the times at which they have occurred (Costa, 2003).

More recently (0.20–1.40 Ma, middle to lower Pleistocene, using a conservative chronological interpolation of divergence dates), *R. v. citreolaemus* evolved separately in the Magdalena valley of Colombia, part of the Nechí area of endemism. Our results suggest that the ancestral population dispersed to the *trans*-Andean region, either from the western lowlands of Amazonia through the Caribbean lowlands, or else by low passes through the Andes (Nores, 2004). Periods of dryer climates possibly separated the proto-*citreolaemus* population evolving at the Nechí area of endemism in Colombia from their counterparts in western Amazonia (Nores, 2004). Although uplift of the Eastern Andes was not the source for the evolution of *R. v. citreolaemus* according to our analysis, these mountains presently act as a relatively effective barrier according to the mean *p*-distance (1.72%) between *R. v. citreolaemus* and its sister clade, composed of the *cis*-Andean taxa *R. v. vitellinus*, *R. v. culminatus* and *R. v. ariel* N (Table 3).

In his analysis of *R. vitellinus* ssp. morphological variation in the hybrid zones, Haffer (1974) suggested that the Serra Pacaraima (central tabular upland of the Guianan shield in Brazil, Venezuela, and Guiana) may act as an important barrier to gene flow between *R. v. vitellinus* and *R. v. culminatus*, and that the lower Amazon river may act as a barrier between *R. v. vitellinus* and *R. v. ariel* N (Fig. 2). The Serra Pacaraima was formed more than 1700 Ma (Santos et al., 2003), so vicariance due to uplift in this region can be ruled out. Better sampling in the Pantepui region (west of the Guianan area, on the northern bank of the Amazon river) is needed to detect possible biogeographic barriers to gene flow. Regarding the Amazon river, the old Amazonian intracratonic basin currently separating the Guianan shield (*R. v. vitellinus*) and Brazilian shield (*R. v. culminatus* + *ariel* N) populations of *R. vitellinus* has been in place since the Paleozoic (Aleixo and Rossetti, 2007), well before it became filled by the course of the modern Amazon river during the Quaternary (Rossetti et al., 2005), and hence is too old to explain the recent split between those two phylogroups (0.20–0.47 Ma, middle Pleistocene). However, the Amazon River is presently an effective barrier to gene flow because we found no evidence of introgression of *R. vitellinus* ssp. haplotypes between the Guiana area of endemism (northern bank) and the Belém and Rondônia areas of endemism (southern bank; Fig. 5a).

Aleixo and Rossetti (2007) found a spatial pattern of diversification in which populations of those centers of endemism associated with the Guianan (Guiana area) and Brazilian shields (Belém and Rondônia areas) were monophyletic, whereas those associated with the western sedimentary basins (Inambari and Napo areas) were not. The sample *R. v. culminatus* 1 from northeastern Inambari (locality 12 in Fig. 2) groups with populations of the Brazilian shield farther to the east rather than with other populations from the same center of endemism (Fig. 5a). This pattern also was observed in the *Xiphorhynchus spixii*/*elegans* woodcreeper species complex (Aleixo, 2004) and indicates that the Inambari area may be a composite center of endemism, and that its northeastern part

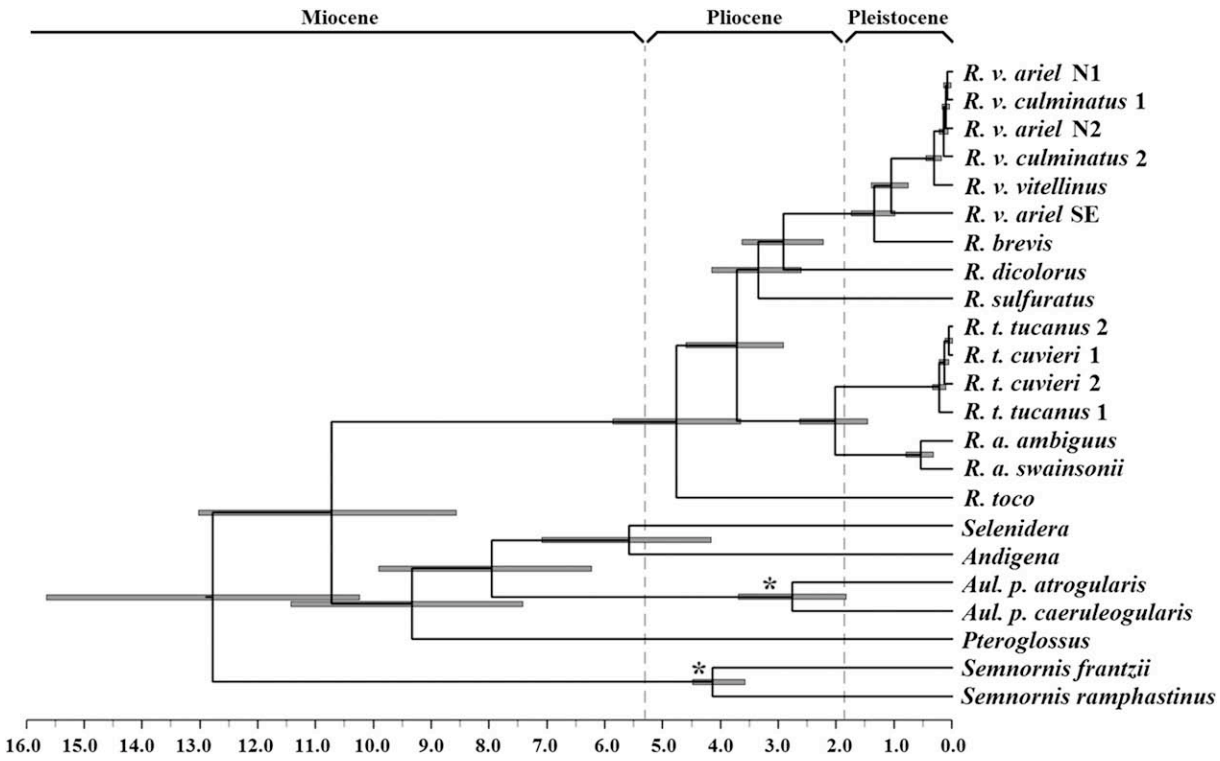

Fig. 6. Chronogram of Bayesian divergence times, with horizontal bars indicating 95% posterior age intervals. Asterisks mark the calibration nodes. *R.* = *Ramphastos*; *Aul.* = *Aulacorhynchus*; *a.* = *ambiguus*; *p.* = *prasinus*; *t.* = *tucanus*; *v.* = *vitellinus*.

is linked biogeographically to the Brazilian shield rather than the neighboring western sedimentary basins. On the other hand, the timing of *R. vitellinus* spp. diversification in Amazonia is too recent to be explained by the vicariant events invoked as causes of the general spatial pattern of diversification described by Aleixo and Rossetti (2007). Since the diversification of *R. vitellinus* spp. in the Amazon took place during the middle and late Pleistocene (Fig. 6), more thorough geographic sampling across the region coupled with niche modeling analyses is needed to better understand historical interactions in these lineages, by evaluating the spatial concordance between the distribution of putative Pleistocene refugia and phylogroups (see Peterson and Nyári, 2008).

Haffer's (1974) analysis, which demonstrates that populations of *R. v. vitellinus*, *R. v. culminatus*, and *R. v. ariel* N are connected through extensive zones of morphological intergradation (Fig. 2), combined with our molecular phylogenetic analyses supporting absence of reciprocal monophyly (Figs. 3 and 5a) and recent diversification (Fig. 6), imply that no barrier except the lower Amazon River (between *R. v. vitellinus* and *R. v. ariel* N) completely prevents gene flow between these taxa. Our results suggest the possibility that dispersal could have taken place in a counter clock-wise direction around the headwaters of the Amazon river, from the Napo and Inambari centers of endemism south and eastwards, since splits related to the southwestern Amazonian haplotypes are more basal in comparison to the haplotypes from eastern Amazonia (Rondônia and Belém areas of endemism; Fig. 5a), although bootstrap support for many of these nodes is low (which is expected in the case of introgression). The *R. vitellinus* ssp. tree topology (Fig. 5a) is congruent with the topology for many Neotropical non-Passeriformes obtained by Borges (2007) using parsimony analysis of endemicity (Fig. 5b). What is not clear is whether or not these patterns are the result of divergence during the same time periods.

The split of the two extant yelper species, *R. ambiguus* and *R. tucanus* (1.48–2.66 Ma) may be associated with the late Tertiary glaciation cycles. This time frame indicates that the Andes was not the source of vicariance, though it may have been important at maintaining differentiation according to the mean inter-taxonomic *p*-distance between *R. tucanus* and *R. ambiguus* (4.52%). *R. tucanus* ssp. (*R. t. tucanus* and *R. t. cuvieri*) had relatively undifferentiated *p*-distances (Table 3) and lacked reciprocal monophyly with respect to one another (Figs. 3a and 6). The divergence time ranges for *R. tucanus* haplotypes (0.12–0.35 Ma) and *R. v. vitellinus*/*R. v. culminatus* + *ariel* N (0.20–0.47 Ma) overlap in the middle Pleistocene, and therefore it is possible that the same biogeographic events affected diversification in both *R. tucanus* and Amazonian *R. vitellinus* groups.

Further population level studies should include samples from (1) *R. tucanus* and Amazonian *R. vitellinus* from the Pantepui and/or Imeri area (northern bank of Amazon river, between the Guiana area of endemism and western Amazonia); (2) the disjunct northeastern Atlantic Forest population of *R. v. ariel* (Fig. 2), to assess how it relates to the SE (southern Atlantic forest) and N (Amazonian) populations (Fig. 2); and (3) *R. vitellinus* samples from central Brazil ("*R. v. pintoi*", Fig. 2), which consists of a defined zone of intergradation between *R. v. culminatus* and *R. v. ariel* N (Haffer, 1974).

5. Conclusions

We took into account uncertainties in both ages and rates by using a relaxed-clock approach to date nodes in the *Ramphastos* phylogeny. The analysis indicated that most ramphastid genera evolved in the late to middle Miocene, *Ramphastos* species throughout the Pliocene and early Pleistocene, and all intra-specific divergences originated in the Pleistocene, which is consistent with other estimates (Aleixo and Rossetti, 2007; Antonelli et al., in press, and references therein). We found relatively high rates of molecular evolution for protein-coding mitochondrial genes (COI,

cyt-*b* and ND2), with only COI embracing the standard "2% mean rate" reported for birds in the literature (García-Moreno, 2004; Lovette, 2004). Our results agree with the findings of Weir and Schluter (2008) that Piciformes (the order to which Ramphastidae belongs) may have accelerated rates for mtDNA protein-coding loci on the order of 4% s/s/Ma.

Contrasting with these estimates of faster rates in Piciformes are the data within other Amazonian lineages. The two widespread lineages of *tucanus* and *vitellinus* share their broad lowland forest distribution with a host of other bird lineages. There are now a number of examples of such lineages having substantially greater genetic structure and divergence in similar mitochondrial markers (e.g., *Glyphorynchus spirurus*, Marks et al., 2002; *Hypocnemis cantator*, Tobias et al., 2008; *Mionectes oleagineus*, Miller et al., 2008; *Schiffornis turdinus*, Peterson and Nyári, 2008). Armenta et al. (2005) found substantially more genetic structure (and divergence) across Amazonia in another ramphastid group, the barbet *Capito niger*. The low levels of genetic divergence across Amazonia in *Ramphastos* are mirrored by data for the piping-guans *Pipile* spp. (Grau et al., 2005) and the parrot *Amazona ochrocephala* (Eberhard and Bermingham, 2004). The toucans, *Pipile* piping-guans, and *Amazona* parrots are large canopy dwelling species with much better dispersal capabilities than the more genetically differentiated species mentioned above. Thus, dispersal abilities likely play an important role in these comparatively lower levels of genetic divergence and cladogenesis of *Ramphastos* lineages across the lowlands, as shown recently for several other Neotropical avian lineages (Burney and Brumfield, 2009).

Acknowledgments

A. Wajntal supervised J.S.L. Patané during his PhD and contributed with helpful suggestions. L.F. Silveira obtained important specimens for this project. We also thank D. Dittmann and F.H. Sheldon (Louisiana State University Museum of Natural Sciences), D.C. Oren (Museu Paraense Emilio Goeldi), M. Robbins (University of Kansas Museum of Natural History), S. Hackett and D. Willard (Field Museum of Natural History), and L. Joseph (Academy of Natural Sciences), who generously loaned tissues for this project. K. Feldheim and E. Sackett provided assistance in the Pritzker laboratory (FMNH). C. Miyaki (LGEMA Lab., USP) provided research support and important *Ramphastos* samples. S.L. Pereira helped with useful comments on analyses. F. d'Horta, G.S. Cabanne, and L.S. Rocha commented on the manuscript. This work was supported by FAPESP, CNPq, National Science Foundation Grant DEB-0515672 to J.D.W., J.M.B., and A.A. and the John D. and Catherine T. MacArthur Foundation funding of the Biodiversity Synthesis Group of the Encyclopedia of Life. DNA sequencing for this project was carried out in part at the Field Museum's Pritzker Laboratory for Molecular Systematics and Evolution, operated with support of the Pritzker Foundation.

References

Abratis, M., Worner, G., 2001. Ridge collision, slab-window formation, and the flux of Pacific asthenosphere into the Caribbean realm. Geology 29, 127–130.
Aleixo, A., 2004. Historical diversification of a "terra-firme" forest bird superspecies: a phylogeographic perspective on the role of different hypotheses of Amazonian diversification. Evolution 58, 1303–1317.
Aleixo, A., Rossetti, D.F., 2007. Avian gene trees, landscape evolution and geology: towards a modern synthesis of Amazonian historical biogeography? J. Ornithol. 148, S443–S453.
Andrade-Lima, D., 1982. Present-day forest refuges in Northeastern Brazil. In: Prance, G.T. (Ed.), Biological Diversification in the Tropics. Columbia Univ. Press, New York, pp. 245–251.
Antonelli, A., Quijada-Mascareñas, A., Crawford, A.J., Bates, J.M., Velazco, P.M., Wüster, W. (in press). Molecular studies and phylogeography of Amazonian tetrapods and their relation to geological and climatic models. In: Hoorn, C., Vonhof, H., Wesselingh, F. (Eds.), Amazonia, Landscape and Species Evolution, Wiley-Blackwell, New York, pp. 386–404.
Armenta, J.K., Weckstein, J.D., Lane, D.F., 2005. Geographic variation in mitochondrial DNA sequences of an Amazonian non-passerine: the Black-spotted Barbet (*Capito niger*). Condor 107, 527–536.
Auler, A.S., Wang, X., Edwards, R.L., Cheng, H., Cristalli, P.S., Smart, P.L., Richards, D.A., 2004. Paleoenvironments in semi-arid northeastern Brazil inferred from high precision mass spectrometric speleothem and travertine ages and the dynamics of South American rainforests. Speleogenesis Evol. Karst Aquifers 2, 1–4.
Barker, F.K., Lanyon, S.M., 2000. The impact of parsimony weighting schemes on inferred relationships among toucans and Neotropical barbets (Aves: Piciformes). Mol. Phylogenet. Evol. 15, 215–234.
Bates, H.W., 1863. The Naturalist on the River Amazon. John Murray, London.
Bates, J.M., Cracraft, J., Hackett, S.J., 1998. Area-relationships in the Neotropical lowlands: an hypothesis based on raw distributions of Passerine birds. J. Biogeogr. 25, 783–793.
Bigarella, J.J., Andrade-Lima, D., Riehs, P.J., 1975. Considerações a respeito das mudanças paleoambientais na distribuição de algumas espécies vegetais e animais no Brasil. An. Acad. Bras. Cienc. 47, 411–464.
Borges, S.H., 2007. Análise biogeográfica da avifauna da região oeste do baixo Rio Negro, amazônia brasileira. Rev. Bras. Zool. 24, 919–940.
Brown, G.G., Gadaleta, G., Pepe, G., Saccone, C., Sbisà, E., 1986. Structural conservation and variation in the D-loop containing region of vertebrate mitochondrial DNA. J. Mol. Biol. 192, 503–511.
Burney, C.W., Brumfield, R.T., 2009. Ecology predicts levels of genetic differentiation in Neotropical birds. Am. Nat. 174, 358–368.
Burns, K.J., Naoki, K., 2004. Molecular phylogenetics and biogeography of Neotropical tanagers in the genus *Tangara*. Mol. Phylogenet. Evol. 32, 838–854.
Coates, A.G., Jackson, J.B.C., Collins, L.S., Cronin, T.M., Dowsett, H.J., Bybell, L.M., Jung, P., Obando, J.A., 1992. Closure of the isthmus of Panama: the near-shore marine record of Costa Rica and western Panama. GSA Bull. 104, 814–828.
Costa, L.P., 2003. The historical bridge between the Amazon and the Atlantic forest of Brazil: a study of molecular phylogeography with small mammals. J. Biogeogr. 30, 71–86.
Cracraft, J., Prum, R.O., 1988. Patterns and processes of diversification: speciation and historical congruence in some Neotropical birds. Evolution 42, 603–620.
Cunningham, C.W., 1997. Can three incongruence tests predict when data should be combined? Mol. Biol. Evol. 14, 733–740.
De Germiny, C.G., 1929. Révision du genre *Rhamphastos*. Oiseau 10, 591–604.
De Oliveira, P.E., Barreto, A.M.F., Suguio, K., 1999. Late Pleistocene/Holocene climatic and vegetational history of the Brazilian caatinga: the fossil dunes of the middle São Francisco river. Palaeogeogr. Palaeoclimatol. Palaeoecol. 152, 319–337.
Delport, W., Ferguson, J.W.H., Bloomer, P., 2002. Characterization and evolution of the mitochondrial DNA control region in hornbills (Bucerotiformes). J. Mol. Evol. 54, 794–806.
Drummond, A.J., Rambaut, A., 2007. BEAST: Bayesian evolutionary analysis by sampling trees. BMC Evol. Biol. 7, 214. doi:10.1186/1471-2148-7-214
Drummond, A.J., Ho, S.Y.W., Phillips, M.J., Rambaut, A., 2006. Relaxed phylogenetics and dating with confidence. PLoS Biol. 4, 699–710.
Duque-Caro, H., 1990. Neogene stratigraphy, paleoceanography and paleobiogeography in northwest South America and the evolution of the Panama Seaway. Palaeogeogr. Palaeoclimatol. Palaeoecol. 77, 203–234.
Eberhard, J.R., Bermingham, E., 2004. Phylogeny and biogeography of the *Amazona ochrocephala* (Aves: Psittacidae) complex. Auk 121, 318–332.
Eberhard, J.R., Bermingham, E., 2005. Phylogeny and comparative biogeography of *Pionopsitta* parrots and *Pteroglossus* toucans. Mol. Phylogenet. Evol. 36, 288–304.
Espinosa de los Monteros, A., 2003. Models of the primary and secondary structure of the 12S RNA of birds: a guideline for sequence aligning. DNA Sequence 14, 241–256.
Farías, M., Charrier, R., Carretier, S., Martinod, J., Fock, A., Campbell, D., Cáceres, J., Comte, D., 2008. Late Miocene high and rapid surface uplift and its erosional response in the Andes of central Chile (33°–35°S). Tectonics 27, TC1005. doi:10.1029/2006TC002046.
Farris, J.S., Källersjö, M., Kluge, A.G., Bult, C., 1994. Testing significance of incongruence. Cladistics 10, 315–319.
Galetti, M., Laps, R., Pizo, M.A., 2000. Frugivory by toucans (Ramphastidae) at two altitudes in the Atlantic Forest of Brazil. Biotropica 32, 842–850.
García-Moreno, J., 2004. Is there a universal mtDNA clock for birds? J. Avian Biol. 35, 465–468.
Gernhard, T., 2008. The conditioned reconstructed process. J. Theor. Biol. 253, 769–778.
Goeldi, E.A., 1894. Aves do Brasil, 1ª Parte. Livraria Clássica de Alves & Cia, Rio de Janeiro.
González, M.A., Eberhard, J.R., Lovette, I.J., Olson, S.L., Bermingham, E., 2003. Mitochondrial DNA phylogeography of the bay wren (Troglodytidae: *Thryothorus nigricapillus*) complex. Condor 105, 228–238.
Gould, J., Rutgers, A., 1972. Birds of South America. Eyre Methuen, London.
Gradstein, F.M., Ogg, J.G., Smith, A.G., Bleeker, W., Lourens, L.J., 2004. A new geologic time scale, with special reference to Precambrian and Neogene. Episodes 27, 83–100.
Grafe, K., Frisch, W., Villa, I.M., Meschede, M., 2002. Geodynamic evolution of southern Costa Rica related to low-angle subduction of the Cocos Ridge: constraints from thermochronology. Tectonophysics 348, 187–204.

Grau, E.T., Pereira, S.L., Silveira, L.F., Höfling, E., Wajntal, A., 2005. Molecular phylogenetics and biogeography of Neotropical piping guans (Aves: Galliformes): *Pipile* Bonaparte, 1856 is synonym of *Aburria* Reichenbach, 1853. Mol. Phylogenet. Evol. 35, 637–645.

Hackett, S.J., 1996. Molecular phylogenetics and biogeography of tanagers in the genus *Ramphocelus* (Aves). Mol. Phylogenet. Evol. 5, 368–382.

Hackett, S.J., Lehn, C.A., 1997. Lack of genetic divergence in a genus of Neotropical birds (*Pteroglossus*): the connection between life-history characteristics and levels of genetic divergence. Ornithol. Monogr. 48, 267–280.

Hackett, S.J., Kimball, R.T., Reddy, S., Bowie, R.C.K., Braun, E.L., Braun, M.J., Chojnowski, J.L., Cox, W.A., Han, K.-L., Harshman, J., Huddleston, C.J., Marks, B.D., Miglia, K.J., Moore, W.S., Sheldon, F.H., Steadman, D.W., Witt, C.C., Yuri, T., 2008. A phylogenomic study of birds reveals their evolutionary history. Science 320, 1763–1768.

Haffer, J., 1974. Avian speciation in tropical South America, vol. 14. Publications of the Nuttall Ornithological Club, Cambridge, Massachusetts.

Haffer, J., 1997. Alternative models of vertebrate speciation in Amazonia: an overview. Biodivers. Conserv. 6, 451–476.

Hafner, M.S., Sudman, P.D., Villablanca, F.X., Spradling, T.A., Demastes, J.W., Nadler, S.A., 1994. Disparate rates of molecular evolution in cospeciating hosts and parasites. Science 265, 1087–1090.

Helm-Bychowski, K., Cracraft, J., 1993. Recovering phylogenetic signal from DNA sequences: relationships within the Corvine assemblage (class Aves) as inferred from complete sequences of mitochondrial cytochrome-*b* gene. Mol. Biol. Evol. 10, 1196–1214.

Höfling, E., 1998. Comparative cranial anatomy of Ramphastidae and Capitonidae. Ostrich 69, 389.

Höfling, E., Alvarenga, H.M.F., 2001. Osteology of the shoulder girdle in the Piciformes, Passeriformes and related groups of birds. Zool. Anz. 240, 196–208.

Hovikoski, J., Gingras, M., Räsänen, M., Rebata, L.A., Guerrero, J., Ranzi, A., Melo, J., Romero, L., del Prado, H.N., Jaimes, F., Lopez, S., 2007. The nature of Miocene Amazonian epicontinental embayment: high-frequency shifts of the low-gradient coastline. Geol. Soc. Am. Bull. 119, 1506–1520.

Huelsenbeck, J.P., Ronquist, F., 2005. Bayesian analysis of molecular evolution using MrBayes. In: Nielsen, R. (Ed.), Statistical Methods in Molecular Evolution. Springer Science + Business Media, Inc., New York, pp. 183–232.

Hurlbert, S.H., 1984. Pseudoreplication and the design of ecological field experiments. Ecol. Monogr. 54, 187–211.

Ibaraki, M., 1997. Closing of the Central American seaway and Neogene coastal upwelling along the Pacific coast of South America. Tectonophysics 281, 99–104.

Ibaraki, M., 2002. Responses of planktonic foraminifera to the emergence of the Isthmus of Panama. Rev. Mex. Cienc. Geol. 19, 152–160.

Jacobs, B.F., Kingston, J.D., Jacobs, L.L., 1999. The origin of grass-dominated ecosystems. Ann. Mo. Bot. Gard. 86, 590–643.

Jobb, G., von Haeseler, A., Strimmer, K., 2004. TREEFINDER: a powerful graphical analysis environment for molecular phylogenetics. BMC Evol. Biol. 4. doi:10.1186/1471-2148-4-18.

Keigwin, L.D.Jr., 1978. Pliocene closing of the isthmus of Panama, based on biostratigraphic evidence from nearby Pacific Ocean and Caribbean Sea cores. Geology 6, 630–634.

Keigwin, L.D.Jr., 1982. Neogene planktonic foraminifers from Deep Sea Drilling Project Sites 502 and 503. Init. Rep. DSDP 68, 269–288.

Kimura, R.K., Pereira, S.L., Grau, E.T., Höfling, E., Wajntal, A., 2004. Genetic distances and phylogenetic analysis suggest that *Baillonius* Cassin, 1867 is a *Pteroglossus* Illiger, 1811. Ornitol. Neotrop. 15, 527–537.

Kocher, T.D., Thomas, W.K., Meyer, A., Edwards, S.V., Pääbo, S., Vallablanca, F.X., Wilson, A.C., 1989. Dynamics of mitochondrial DNA evolution in animals: amplification and sequencing with conserved primers. Proc. Natl. Acad. Sci. USA 86, 6196–6200.

Kumar, S., Tamura, K., Nei, M., 2004. MEGA 3: integrated software for molecular evolutionary genetics analysis and sequence alignment. Brief. Bioinform. 5, 150–163.

Lanyon, S.M., Zink, R.M., 1987. Genetic variation in piciform birds: monophyly and generic and familial relationships. Auk 104, 724–732.

Latorre, C., Quade, J., McIntosh, W.C., 1997. The expansion of C4 grasses and global change in the late Miocene: stable isotope evidence from the Americas. Earth Planet. Sci. Lett. 146, 83–96.

Lovette, I.J., 2004. Mitochondrial dating and mixed support for the "2% rule" in birds. Auk 121, 1–6.

Maddison, W.P., Maddison, D.R., 2009. Mesquite: a modular system for evolutionary analysis. Version 2.6 - http://mesquiteproject.org.

Marks, B.D., Hackett, S.J., Capparella, A.P., 2002. Historical relationships among Neotropical lowland forest areas of endemism as determined by mitochondrial DNA sequence variation within the Wedge-billed Woodcreeper (Aves: Dendrocolaptidae: *Glyphorynchus spirurus*). Mol. Phylogenet. Evol. 24, 153–167.

Meyer de Schauensee, R., 1966. The species of birds of South America with their distribution. Livingston Publishing, Narberth, Pennsylvania.

Meyer de Schauensee, R., 1970. A Guide to the Birds of South America. Livingston Publishing, Wynnewood, Pennsylvania.

Miller, M.J., Bermingham, E., Klicka, J., Escalante, P., Raposo do Amaral, F., Wier, J.T., Winker, K., 2008. Out of Amazonia again and again: episodic crossing of the Andes promotes diversification in a lowland forest flycatcher. Proc. R. Soc. B 275, 1133–1142.

Miyaki, C.M., Matioli, S.R., Burke, T., Wajntal, A., 1998. Parrot evolution and paleogeographical events: mitochondrial DNA evidence. Mol. Biol. Evol. 15, 544–551.

Mori, S.A., 1989. Eastern, extra-Amazonian Brazil. In: Campbell, D.G., Hammond, D. (Eds.), Floristic Inventory of Tropical Countries. The New York Botanical Gardens, New York, pp. 428–454.

Moyle, R.G., 2004. Phylogenetics of barbets (Aves: Piciformes) based on nuclear and mitochondrial DNA sequence data. Mol. Phylogenet. Evol. 30, 187–200.

Nahum, L.A., Pereira, S.L., Fernandes, F.M.C., Matioli, S.R., Wajntal, A., 2003. Diversification of Ramphastinae (Aves, Ramphastidae) prior to the Cretaceous/Tertiary boundary as shown by molecular clock of mtDNA sequences. Genet. Mol. Biol. 26, 411–418.

Nambudiri, E.M.V., Tidwell, W.D., Smith, B.N., Hebbert, N.P., 1978. A C4 plant from the Pliocene. Nature 276, 816–817.

Nores, M., 2004. The implications of Tertiary and Quaternary sea level rise events for avian distribution patterns in the lowlands of northern South America. Global Ecol. Biogeogr. 13, 149–161.

Pereira, S.L., Grau, E.T., Wajntal, A., 2004. Molecular architecture and rates of DNA substitutions of the mitochondrial control region of cracid birds. Genome 47, 535–545.

Peters, J.L., 1948. Check-List of Birds of the World, vol. 6. Harvard University Press, Cambridge, Massachusetts.

Peterson, A.T., Nyári, A.S., 2008. Ecological niche conservatism and Pleistocene refugia in the Thrush-like Mourner *Schiffornis* sp., in the Neotropics. Evolution 62, 173–183.

Posada, D., Buckley, T.R., 2004. Model selection and model averaging in phylogenetics: advantages of Akaike information criterion and Bayesian approaches over likelihood ratio tests. Syst. Biol. 53, 793–808.

Posada, D., Crandall, K.A., 1998. Modeltest: testing the model of DNA substitution. Bioinformatics 14, 817–818.

Prum, R.O., 1988. Phylogenetic interrelationships of the barbets (Aves: Capitonidae) and toucans (Aves: Ramphastidae) based on morphology with comparisons to DNA-DNA hybridization. Zool. J. Linn. Soc. 92, 313–343.

Prychitko, T.M., Moore, W.S., 1997. The utility of DNA sequences of an intron from the beta-fibrinogen gene in phylogenetic analysis of woodpeckers (Aves: Picidae). Mol. Phylogenet. Evol. 8, 193–204.

Rambaut, A., Drummond, A.J., 2008. Tracer version 1.4.

Ribas, C.C., Gaban-Lima, R., Miyaki, C.Y., Cracraft, J., 2005. Historical biogeography and diversification within the Neotropical Parrot genus *Pionopsitta* (Aves: Psittacidae). J. Biogeogr. 32, 1409–1427.

Ronquist, F., Huelsenbeck, J.P., 2003. MrBayes 3: Bayesian phylogenetic inference under mixed models. Bioinformatics 19, 1572–1574.

Rossetti, D.F., Toledo, P.M., Góes, A.M., 2005. New geological framework for western Amazonia (Brazil) and implications for biogeography and evolution. Quaternary Res. 63, 78–89.

Saccone, C., Pesole, G., Sbisà, E., 1991. The main regulatory region of mammalian mitochondrial DNA: structure–function model and evolutionary pattern. J. Mol. Evol. 33, 83–91.

Saito, T., 1976. Geologic significant of coiling direction in the planktonic foraminifera *Pulleniatina*. Geology 4, 305–309.

Sambrook, J., Russell, D.W., 2001. Molecular Cloning: A Laboratory Manual. Cold Spring Harbor Laboratory Press, New York.

Santos, J.O.S., Potter, P.E., Reis, N.J., Hartmann, L.A., Fletcher, I.R., McNaughton, N.J., 2003. Age, source and regional stratigraphy of the Roraima supergroup and Roraima-like sequences in northern South America, based on U-Pb Geochronology. Geol. Soc. Am. Bull. 115, 331–348.

Short, L.L., Horne, J.F.M., 2001. Toucans, Barbets and Honeyguides. Bird Families of the World, vol. 8. Oxford University Press, New York.

Sorenson, M.D., Ast, J.C., Dimcheff, D.E., Yuri, T., Mindell, D.P., 1999. Primers for a PCR based approach to mitochondrial genome sequencing in birds and other vertebrates. Mol. Phylogenet. Evol. 12, 105–114.

Swofford, D.L., 2003. PAUP*: Phylogenetic Analysis Using Parsimony (* and Other Methods). Version 4. Sinauer Associates, Sunderland, Massachusetts.

Tobias, J.A., Bates, J.M., Hackett, S.J., Seddon, N., 2008. Comment on "The latitudinal gradient in recent speciation and extinction rates of birds and mammals". Science 319, 901c.

Van Tyne, J., 1929. The Life History of the Toucan *Ramphastos brevicarinatus*, vol. 19. Univ. of Michigan Museum of Zoology Miscellaneous Publications.

Van Tyne, J., 1955. Evolution in the toucan genus *Ramphastos*. In: Portmann, A., Sutter, E. (Eds.), Acta XI Congressus Internationalis Ornithologici. Birkhaeuser Verlag, Basel, pp. 362–368.

Weckstein, J.D., 2005. Molecular phylogenetics of the *Ramphastos* toucans: implications for the evolution of morphology, vocalizations, and coloration. Auk 122, 1191–1209.

Weir, J.T., Schluter, D., 2008. Calibrating the avian molecular clock. Mol. Ecol. 17, 2321–2328.

Wesselingh, F.P., Räsänen, M.E., Irion, G., Vonhof, H.B., Kaandorp, R., Renema, W., Romero-Pittman, L., Gingras, M., 2001. Lake Pebas: a palaeoecological reconstruction of a Miocene long-lived lake complex in western Amazonia. Cainozoic Res. 1, 35–81.

Willis, E.O., 1992. Zoogeographical origins of eastern brazilian birds. Ornitol. Neotrop. 3, 1–15.